Single-stage Ti:sapphire-pumped deep-infrared optical parametric oscillator based on $CdSiP_2$

Callum F. O'Donnell, S. Chaitanya Kumar, Kevin T. Zawilski, Peter G. Schunemann, and Majid Ebrahim-Zadeh, *Member, IEEE*

We report a high-repetition-rate femtosecond optical parametric oscillator (OPO) for the deep-infrared (deep-IR) based on the nonlinear optical crystal, $CdSiP_2$ (CSP), pumped directly by a Ti:sapphire laser, for the first time. By pumping CSP at <1 μm, we have achieved practical output powers at the longest wavelengths generated by any Ti:sapphire-pumped OPO. Using a combination of pump wavelength tuning, type-I critical phase-matching, and cavity delay tuning, we have generated continuously tunable radiation across 6654–8373 nm (1194–1503 cm^{-1}) at 80.5 MHz repetition rate, providing up to 20 mW of average power at 7314 nm and >7 mW beyond 8000 nm, with idler spectra exhibiting bandwidths of 140–180 nm across the tuning range. Moreover, the near-IR signal is tunable across 1127–1192 nm, providing up to 37 mW of average power at 1150 nm. Signal pulses, characterised using intensity autocorrelation, have durations of ~260–320 fs, with corresponding time-bandwidth product of $\Delta\upsilon\Delta\tau$~1. The idler and signal output exhibit a TEM_{00} spatial profile with single-peak Gaussian distribution. With an equivalent spectral brightness of ~6.68×10^{20} photons s^{-1} mm^{-2} sr^{-1} 0.1% BW^{-1}, this OPO represents a viable alternative to synchrotron and supercontinuum sources for deep-IR applications in spectroscopy, metrology and medical diagnostics.

I. Introduction

For as long as infrared spectroscopy has been practised, the spectral region from 4–12 μm in the mid-infrared (mid-IR) to deep-infrared (deep-IR) has been of utmost interest due to the presence of strong absorption peaks corresponding to the fundamental vibrational modes of numerous common molecules [1]. Where these peaks coincide with the atmospheric transmission windows across 3-5 μm and ~7.5–12 μm, there exists the possibility to easily and unambiguously identify the concentrations of individual compounds through the strength of their molecular fingerprint. Today, there is a wide range of applications based upon this principle, including microscopy, security, medical imaging and surgery [2-5]. The workhorse for such applications has long been Fourier Transform Infrared Spectroscopy (FTIR), involving the illumination of a sample using a broadband IR source such as a globar. Although the spectral coverage is broad, the diffuse and incoherent nature of the light source places limitations on the achievable spatial resolution and signal-to-noise ratio [6].

In the absence of conventional solid-state lasers at these wavelengths, a variety of different approaches towards the development of high-power coherent mid-IR and deep-IR sources have been explored. The high average power and spectral brightness of a synchrotron source is one solution, but with the disadvantage of large size, requirement for in-situ measurements, and restricted beam time. Quantum cascade lasers are available across the mid-IR and deep-IR, however, the inability to generate pulses shorter than a few nanoseconds limits their peak power, and the attainment of wide tunability requires multiple laser chips [7]. Broad spectral coverage can be obtained from supercontinuum sources, albeit at low spectral intensity, while reaching the crucial wavelengths requires powerful pump sources in the mid-IR, increasing cost and complexity [8]. On the other hand, nonlinear parametric down-conversion techniques can exploit well-established near-IR solid-state and fibre laser technology to generate powerful coherent radiation far into the infrared [9]. Furthermore, the temporal qualities of the pump laser are transferred to the down-converted beams, enabling high-repetition-rate quasi-continuous-wave pulse trains with kW level peak power. Such sources are most commonly realised using difference-frequency-generation (DFG), optical parametric generation (OPG) or optical parametric oscillators (OPOs) based on suitable mid-IR nonlinear crystals. In such processes, varying the crystal refractive index or input beam wavelength enables single device tuning over a very broad spectral range. The DFG process has the advantage of a single-pass arrangement, but two pump sources closely spaced in wavelength are required to reach the deep-IR. By performing DFG between the signal and idler of OPOs synchronously pumped by Ti:sapphire or Yb fiber laser, or using seeded optical parametric amplifiers (OPAs), milliwatt-level average power femtosecond pulses have been produced across 4–12

This work was supported in part by the Spanish Ministry of Economy and Competitiveness (MINECO) (nuOPO, TEC2015-68234-R); European Commission (Project Mid-Tech, H2020-MSCA-ITN-2014); European Office of Aerospace Research and Development (EOARD) (FA9550-14-1-0390); CERCA Programme/Generalitat de Catalunya; Severo Ochoa Programme for Centres of Excellence in R&D (SEV-2015-0522); Fundació Privada Cellex. Callum. F. O'Donnell acknowledges the support of Marie Curie Actions: Innovative Training Network through the Mid-Tech project (H2020-MSCA-ITN-2014).

Callum F. O'Donnell is with Radiantis, 08850 Gavà, Barcelona, Spain and ICFO-Institut de Ciencies Fotoniques, 08860 Castelldefels, Barcelona, Spain. (email: callum.odonnell@radiantis.com)
S. Chaitanya Kumar is with Radiantis, 08850 Gavà, Barcelona, Spain. (email: chaitanya.suddapalli@radiantis.com)
Kevin T. Zawilski is with BAE Systems Inc., PO Box. 868, Nashua, New Hampshire, USA (email: kevin.zawilski@baesystems.com)
Peter G. Schunemann is with BAE Systems Inc., PO Box. 868, Nashua, New Hampshire, USA (email: peter.g.schunemann@baesystems.com)
M. Ebrahim-Zadeh is with ICFO-Institut de Ciencies Fotoniques, 08860 Castelldefels, Barcelona, Spain, and also with Institucio Catalana de Recerca i Estudis Avancats, 08010, Barcelona, Spain (e-mail: majid.ebrahim@icfo.eu)

μm [10,11]. However, this method incorporates two frequency conversion stages, leading to a costly setup and low overall efficiency. While commercial OPOs are capable of directly producing hundreds of milliwatts of average power up to 4.5 μm in the mid-IR, efforts to advance their wavelength access into the deep-IR have been hampered by stringent nonlinear crystal requirements. The necessary material properties include a high nonlinear coefficient, d_{eff}, resistance to damage at high optical intensities, bulk transparency, and ability to be phase-matched at the desired pump, signal and idler wavelengths.

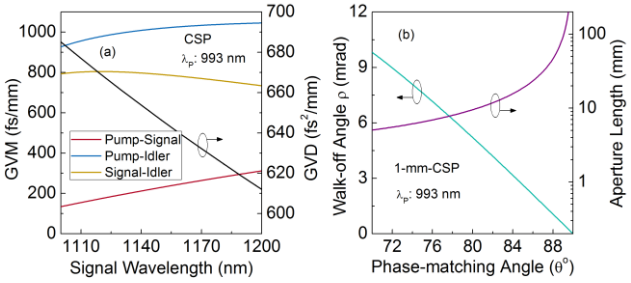

Fig. 1. (a) GVM between the pump at 993 nm, signal and idler, and GVD across 1100–1200 nm. (b) Spatial walk-off and aperture length for a phase-matching angle from θ=70° to 90°.

The search for nonlinear crystals which simultaneously satisfy all criteria has been challenging; oxide-based crystals (e.g. $LiNbO_3$, $KTiOPO_4$, $RbTiOAsO_4$, $CsTiOAsO_4$) perform well when pumped by ~1 μm lasers, but are limited to output below 4.5 μm by multiphonon absorption. On the other hand, almost all highly nonlinear non-oxide crystals (e.g $AgGaSe_2$, GaAs, $ZnGeP_2$) have a narrow optical bandgap resulting in strong two-photon absorption below 1.5 μm. In general, there has been shown to be a negative correlation between the size of the bandgap and the magnitude of d_{eff} [12]. The breakthrough finally came by the successful development of cadmium silicon phosphide, $CdSiP_2$ (CSP), a chalgocenide crystal which was first grown to sufficient optical quality in 2010 [13]. With a nominal transparency across 1–7 μm, thermal conductivity of 13.6 W/m·K, and d_{eff} ~84 pm/V, it enables single stage conversion from 1.06 μm to the mid-IR and deep-IR [14]. Moreover, its nonlinear figure of merit (FOM=d_{eff}^2/n^3) ranks among the highest of all existing nonlinear crystals. The potential of CSP was first demonstrated through picosecond OPG and OPOs at low repetition rates [15-17], before high-repetition-rate femtosecond OPOs were subsequently reported [18-21]. Fig. 1(a) shows the group velocity mismatch (GVM) between the interacting pump, signal and idler waves, and the signal group velocity dispersion (GVD) across the range 1100–1200 nm, relevant for OPOs pumped near 1 μm. The GVM between pump and signal varies over 134–312 fs²/mm, implying that the effective temporal interaction length is 0.4–1 mm for ~130 fs pulses. In such short crystals, the parametric gain remains very high, due to the large d_{eff} and high peak intensities involved. As a birefringent crystal, under type-I critical phase-matching ($e\rightarrow oo$), the extraordinarily polarised wave will experience a spatial walk-off at angle ρ, leading to an effective parametric interaction length (aperture length) of $l_a=\sqrt{\pi}w_0/\rho$, where w_0 is the beam waist. The magnitude of ρ and l_a for a focused pump beam waist of w_0=28 μm, are shown in Fig. 1(b), as a function of phase-matching angle, θ, for a 1-mm-long crystal under type-I phase-matching ($e\rightarrow oo$) pumped at λ=993 nm. As the phase-matching angle is reduced from θ=90° to 70°, the aperture length decreases down to ~5 mm. Therefore, even at large crystal rotation angles, the spatial walk-off does not become a limiting factor for parametric generation.

The emergence of femtosecond mode-locked Yb, Er, and Tm fiber lasers at ~1 μm, ~1.56 μm and ~2 μm, respectively, has greatly expanded the repertoire of suitable pump sources, finally enabling direct pumping of the established IR crystals $AgGaSe_2$ and OP-GaAs. Together with the genesis of CSP, and even more recently, orientation-patterned GaP (OP-GaP), the past few years have seen numerous breakthroughs in the field of single-stage deep-IR frequency conversion, the extent of which are summarised in Table I.

TABLE I
FEMTOSECOND MID-IR AND DEEP-IR SINGLE-STAGE OPOS

Pump	Rep. rate (MHz)	Crystal	Tuning method[a]	Idler (μm)[b]	Pump power (**W**) (wavelength (nm))	Idler power (**mW**) (wavelength (μm)[c]	Idler pulse duration (fs)	Ref.
Ti:sapphire	80	CSP	P, A, C	6.7–8.4	**0.83** (993–1011)	**20** (7.3), **7** (8.1)	~300 (est.)	This work
Yb:KGW	43	CSP	C	6.8–7.0	**5** (1029)	**110** (7.0)	~500 (est.)	[19]
Er fibre laser	100	$AgGaSe_2$	A	4.8–6.0	**0.3** (1560)	**18** (5.0)	~180	[23]
Ti:sapphire	84	MgO:PPLN	Q, C	2.8–6.8	**1.5** (810)	**11** (5.3), **0.2** (6.5)	~150 (est.)	[25]
Yb fibre laser	100	OP:GaP	Q	5.0–12	**2** (1040)	**55** (5.0), **15** (8.5), **7.5** (12)	≥150	[24]
Tm fibre laser	75	OP:GaAs	-	4.1 (2.6 – 6.1 bandwidth)	**1** (2050)	**37** (2.6–6.1 bandwidth)	≥93	[22]

[a]Tuning methods: P: Pump tuning, A: Angle tuning, C: Cavity delay tuning, Q: QPM grating tuning
[b]Range defined relative to weighted centre of most extreme recorded spectra, not 10 dB limit
[c]Peak idler power and power at selected wavelengths of interest

These include a doubly- resonant degenerate OPO based on OP-GaAs pumped by a 93 fs Tm-fibre laser at 2050 nm [22], a CSP-based OPO pumped by a 5 W, 560 fs Yb:KGW solid-state laser at 1029 nm [19], a 300 mW 90 fs Er-fiber-pumped $AgGaSe_2$ OPO [23], and an OP-GaP Yb-fiber-pumped OPO operating at several discrete wavelengths in the deep-IR [24].

In this work, we add another important milestone to this list, by demonstrating a deep-IR femtosecond OPO based on CSP, pumped directly at by a Kerr-lens-mode-locked (KLM) Ti:sapphire laser, for the first time. In doing so, we show that deep-IR radiation can be generated in a single conversion stage using well-established ultrafast pump laser technology.

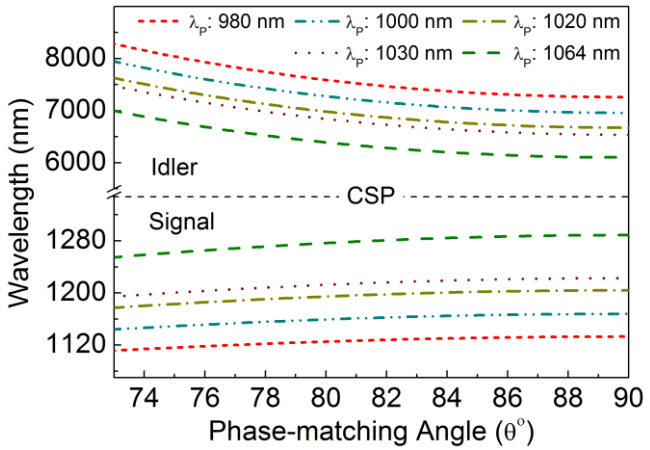

Fig. 2. Signal and idler tuning curves for type-I (*e*→*oo*) critical phase-matching as a function of the CSP internal angle for various pump wavelengths in the range so far used to pump CSP OPOs.

The deployment of the KLM Ti:sapphire laser also offers the important advantage of pump wavelengths <1 μm, which enables the generation of longer idler wavelengths in the deep-IR. This is illustrated in Fig. 2, where the signal and idler wavelength tuning as function of the CSP phase-matching angle under critical type-I (*e*→*oo*) phase-matching for various discrete pump wavelengths of interest, from Yb-based solid-state and fibre lasers down to the Ti:sapphire laser, is presented. As can be clearly seen, for all phase-matching angles (including θ=90° at NCPM), longer deep-IR idler wavelengths can be generated by deploying shorter pump wavelengths in the Ti:sapphire laser wavelength range. The versatility of the KLM Ti:sapphire pump laser, in combination with the excellent optical properties of CSP, enable us to achieve deep-IR tuning across 6654–8373 nm using a combination of pump wavelength tuning, angle tuning under type-I critical phase matching, and cavity delay tuning. We have been able to generate up to 20 mW of deep-IR average power at 7314 nm at 80.5 MHz pulse repetition rate, in TEM_{00} spatial beam quality. Moreover, up to 37 mW is also available in the near-IR signal, with pulse durations measured from 259 to 319 fs. To the best of our knowledge, these results represent the first demonstration of practical powers beyond >7 μm from any Ti:sapphire-laser-pumped OPO with no intermediate frequency conversion stage, and the longest wavelengths generated using CSP to date.

II. Experimental Setup

The configuration of the deep-IR CSP OPO is depicted in Fig. 3. The pump source is a KLM Ti:sapphire laser (Spectra-Physics *Mai Tai HP*), providing near transform-limited ultrashort pulses at a repetition rate of 80.5 MHz. To reduce any two-photon absorption, we operated the laser close to the upper limit of its tuning range (640–1040 nm), where the average output power is >700 mW, comfortably higher than the reported threshold in a CSP OPO pumped close to 1 μm [21]. Using a half-wave plate, we adjusted the polarisation to that required for type-I (*e*→*oo*) in the CSP crystal. The 1-mm-long crystal was cut at θ=90° (ϕ=45°) for noncritical phase matching (NCPM) at normal incidence, and mounted on a precision rotation stage to enable angle tuning. A lens, L_1, of focal length, *f*=100 mm, was used to focus the pump beam to a waist radius of w_0~28 μm, ensuring optimal parametric interaction with the signal without the risk of crystal damage. The OPO cavity is configured in a ring comprising two plano-concave

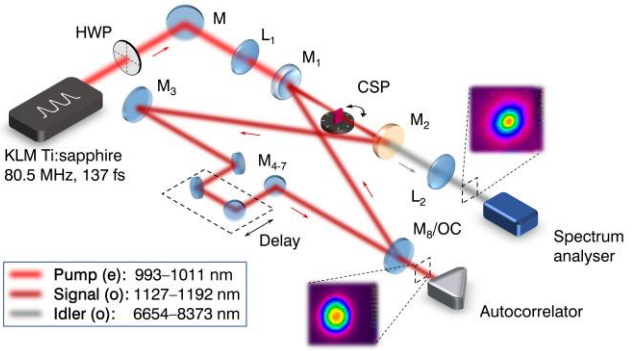

Fig. 3. Schematic of the experimental setup for the Ti:sapphire- pumped CSP femtosecond OPO. HWP: Half wave plate, M: Mirrors, OC: Output coupler, L: Lenses.

TABLE II
Optics and Coatings

Optic	Substrate	High-reflection (nm)	Anti-reflection (nm)
L_1	NBK7	-	650–1050 **(>99%)**
L_2	CaF_2	-	6000–8500 **(>60%)**
M_1	CaF_2	1100–1300 **(>99%)**	990–1015 **(70–83%)**
M_2	ZnSe	1100–1300 **(>97%)**	6500–9000 **(94%)**
$M_{3\text{-}7}$	NBK7	1100–1300 **(>99.8%)**	-
M_8/OC	NBK7	1100–1300 **(>95%)**	-
Crystal	CSP	-	950–1080 **(>99%)** 1100–1200 **(>99%)** 7000–8500 **(>93%)**

mirrors, $M_{1\text{-}2}$ (*r*=100 mm), and six plane mirrors, $M_{3\text{-}8}$, with $M_{5\text{-}6}$ mounted on a translation stage forming a delay line to allow precise control of synchronisation. All cavity mirrors were coated to ensure singly-resonant OPO operation for the near-IR signal, and efficient single-pass extraction of the

deep-IR idler through M_2. Full details of optical coatings are summarised in Table II. M_8 was alternatively used as a signal high-reflector to achieve maximum idler power, and a 5% output coupler was used to enable characterisation of the signal. A lens, L_2, collimates the idler for alignment into a spectrum analyser, while the output-coupled signal is directed to an intensity autocorrelator.

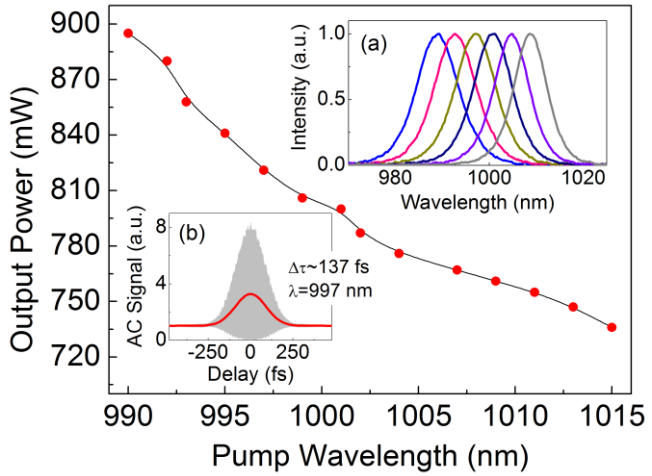

Fig. 4. Ti:sapphire power across 990–1015 nm. Insets: (a) Spectra across tuning range, (b) typical interferometric autocorrelation.

The characteristics of the Ti:sapphire laser used in this experiment over the range 990–1015 nm are shown in Fig. 4. Also shown are the smooth pump spectra and a sample interferometric autocorrelation recorded at 997 nm. The resultant de-convolved pulse duration is 137 fs, which we measured to be constant across the tuning range used in the experiment. The time-bandwidth product of $\Delta\nu\Delta\tau$~0.44 is ~1.4 times higher than the transform limit for *sech*^{2} pulses, this slight chirp is thought to accumulate due to the distance of several metres between autocorrelator and laser aperture, with bounces from several unchirped mirrors. To determine the optimum wavelength for pumping the OPO, transmission measurements of the 1-mm-CSP crystal were performed by focusing the pump beam to a waist radius of w_0~36 μm, with an average power of 500–600 mW, corresponding to a peak intensity of 1.1–1.3 GW/cm^2. Using a power meter and spectrum analyser, we measured transmitted power as a function of Ti:sapphire wavelength for both *ordinary* and *extraordinary* polarisations. The data was recorded over the range 900–1020 nm, with the results shown in Fig. 5. A significant drop in transmission is noted below ~993 nm, in agreement with previous literature which lists the short-wavelength edge as ~1 μm [13]. The pump wavelength choice for the most efficient deep-IR performance is, therefore, a trade-off between absorption losses and pump power, both of which increase towards shorter wavelengths. We found that although the crystal transmission remains ~90% below 993 nm, the subsequent increase in pump power did not enable oscillation. The lower wavelength limit for OPO operation was thus 993 nm, while the upper limit was 1011 nm, beyond which the combination of lower pump power and coating losses in M_1 reduced the available power below threshold. Therefore, in this experiment we were able to pump tune the OPO over 18 nm across 993–1011 nm.

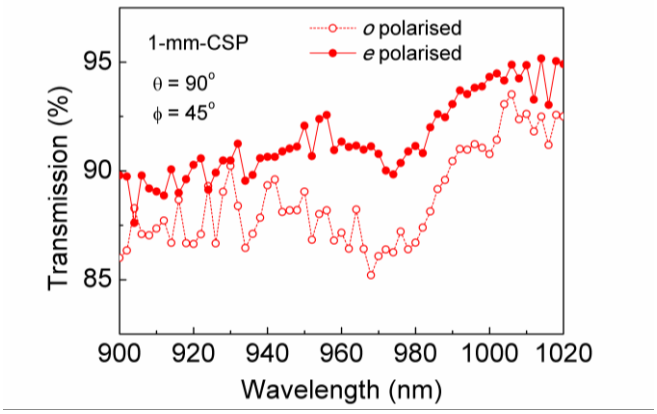

Fig. 5. Transmission of the 1-mm-long CSP across 900–1020 nm for both *ordinary (o)* and *extraordinary (e)* polarisations.

III. Results and Discussion

CSP is known to exhibit detrimental two-photon absorption effects when pumped at high intensities near ~1 μm [18, 19]. To assess the magnitude of these effects, we focused the beam to a waist radius of w_0~37 μm, and recorded the transmitted power as the pump power was steadily increased. The CSP transmission was recorded as a function of input intensity for both *ordinary* (*o*) and *extraordinary* (*e*) polarisations, with the results at the pump wavelength of 993 nm shown in Fig. 6. From the polynomial fit to the experimental data, it can be seen that for both polarisations the relationship becomes increasingly nonlinear at higher input intensities. Although the ratio of the CSP bandgap energy (2.45 eV) to the pump laser photon energy (1.25 eV) results in a value of ~0.51, indicating major contribution from two-photon absorption, the experimental data show additional nonlinear effects, requiring confirmation through further investigation.

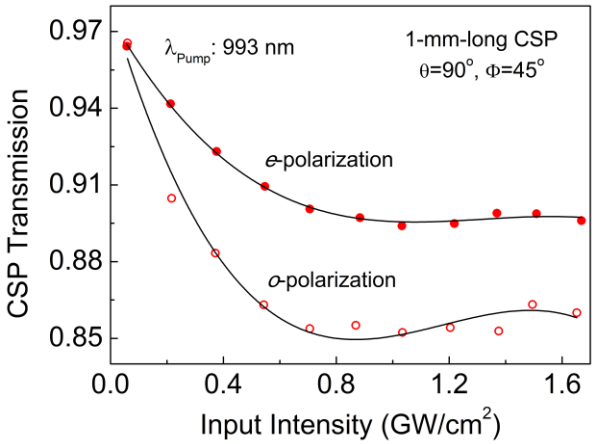

Fig. 6. Transmission measurements of the 1-mm-long CSP crystal at 993 nm for both *ordinary (o)* and *extraordinary (e)* polarisations, at increasing intensities.

Operation of the OPO was achieved by assembling the

cavity as shown in Fig. 2, and synchronisation was obtained by fine adjustment of the delay line. We first performed characterisation by recording the output signal spectrum using a spectrum analyser at different pump wavelengths across the available tuning range. Fig. 7 shows the experimental data for pump tuning superimposed on the parametric gain map, calculated using the Sellmeier equations reported in [13]. For each pump wavelength we set the OPO to perfect synchronisation by maximising the output power with minute adjustments to the cavity length, and recorded the corresponding signal wavelength. In addition, spectra were recorded at the extremes of cavity length detuning, at the positions where oscillation ceased. Since the spectra in each case were highly asymmetric, the central wavelength was determined using a centre-of-mass averaging algorithm.

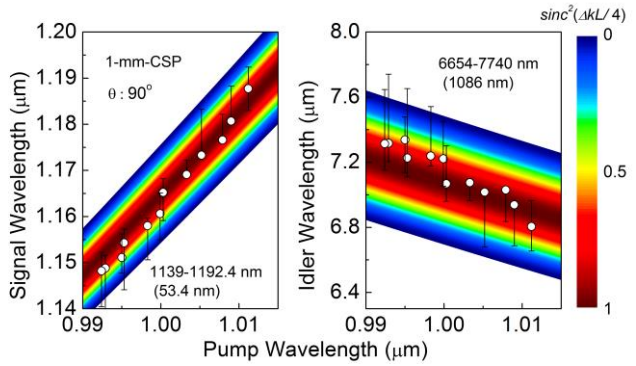

Fig. 7. Pump tuning of the OPO across 993–1011 nm, superimposed on the parametric gain bandwidth for a 1-mm-long crystal.

White spots on Fig. 7 represent the positions at which the highest output power was observed, while the vertical error bars show the extent of additional cavity delay tuning. The data points for the corresponding idler were calculated using energy conservation. We were able to achieve rapid tuning over 1139–1192.4 nm in the signal, and across 6654–7740 nm in the idler using this method. There is generally good agreement between the phase-matching bandwidth and the available cavity delay tuning, however, additional factors that influence the maximum detuning range include cavity dispersion, circulating power, and beam misalignment.

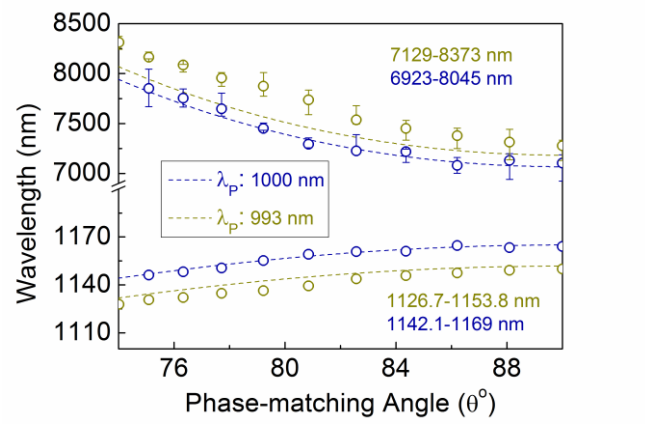

Fig. 8. Idler and signal tuning as a function of the internal phase-matching angle in the CSP crystal, for pump wavelengths of 993 nm and 1000 nm, compared to the wavelength tuning curves predicted using the Sellmeier equations in [13]. Error bars represent additional cavity delay tuning.

In order to generate the longest idler wavelengths, type-I critical phase-matching was employed in the form of crystal rotation from θ=90° to 74°. For each phase-matching angle, the signal spectrum at perfect synchronisation was recorded, and the corresponding deep-IR idler was calculated from the centre wavelength using energy conservation. The results are shown in Fig. 8, where it can be seen that the near-IR signal wavelength could be tuned across 1126.7–1153.8 nm, with the idler covering a spectral range of 6923–8373 nm in the deep-IR, for two pump wavelengths at 993 nm and 1000 nm. The measured values are also compared to the Sellmeier predictions [13], with the observed offset accredited to strong self-phase modulation (SPM) redistributing the spectral density towards shorter wavelengths. It is expected that introducing dispersion control in the form of intracavity prisms or the use of optimised chirped mirrors for the OPO will reduce the discrepancy between the experimental tuning data and the calculations. As seen in Fig. 7 and Fig. 8, the relatively wide parametric gain bandwidth of CSP enables wavelength tuning by variation of cavity length. This is a convenient method for rapid tuning across a large idler bandwidth. An example of cavity delay tuning from this OPO at a pump wavelength of 993 nm and phase-matching angle of 90° is shown in Fig. 9. For a singly-resonant OPO, the rate of change of signal wavelength can be used to acquire an estimate for the total cavity group delay dispersion (GDD), using the relation

$$GDD \equiv \beta_2 L = \frac{{\lambda_s}^2}{2\pi c^2}\left(\frac{d\lambda_s}{dL}\right)^{-1} \qquad (1)$$

Where β_2 is average cavity GVD, L is the total cavity length, λ_s is the signal wavelength, c is the velocity of light, and $d\lambda_s/dL$ is the gradient from Fig. 9.

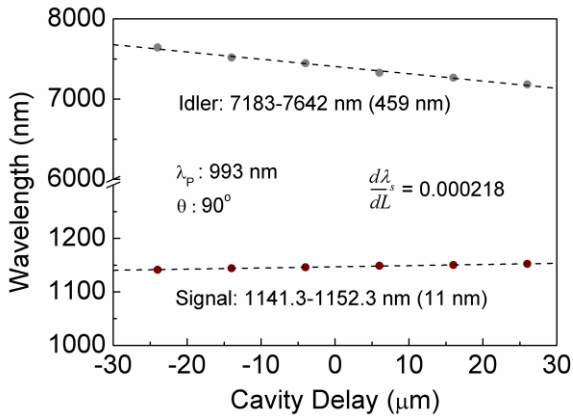

Fig 9. Cavity delay tuning at normal incidence for a pump wavelength of 993 nm.

Evaluating equation (1) for the experimentally measured value of $d\lambda_s/dL$=0.000218 yields an estimated total GDD of ~10700 fs^2. This value is much greater than the expected

contribution from the 1-mm-long CSP crystal, which at 1.15 μm is calculated to be ~646 fs^2, indicating that other cavity elements, such as the uncompensated mirrors M_1, M_2 and M_8, contribute significantly to the total GDD value. Further investigation is required to determine the dominant cause of dispersion. The signal and idler output powers across the tuning range of the CSP femtosecond OPO, are displayed in Fig. 10. Data points below ~7300 nm were acquired using pump tuning with a pump power varying from 430 mW at 1011 nm to 690 mW at 993 nm, after transmission through M_1, while those above were acquired using angle tuning at 993 nm for a fixed pump power of 690 mW.

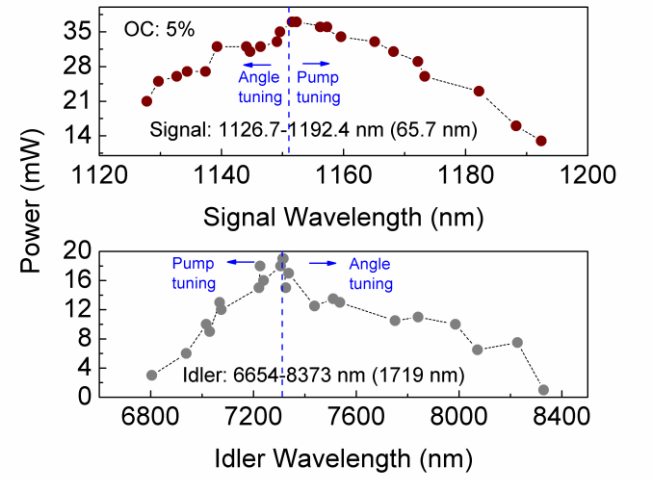

Fig. 10. Signal and idler average powers measured across the total tuning range, using a 5% output coupler to extract the signal.

We extracted deep-IR idler average powers of >10 mW across >65% of the tuning range, with a maximum of 20 mW at 7314 nm and >6 mW available up to 8227 nm. This is equivalent to a peak idler quantum conversion efficiency of 21.3%. Furthermore, with a 5% output coupler in place, we measured signal powers up to 37 mW at 1152 nm. The drop-off in power towards long idler wavelengths is primarily due to Fresnel losses at large crystal rotation angles, while at lower wavelengths it is caused by a reduction in available pump power. It is noted that data here is not corrected for losses in the crystal, mirrors M_2 and M_8, filters $F_{1\text{-}2}$, and a ~40 % transmission loss through L_2.

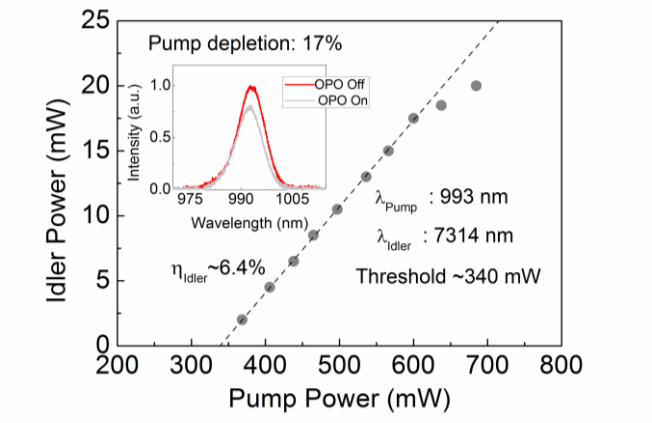

Fig 11. Power scaling of the idler extracted from the CSP femtosecond OPO. Inset: Input pump spectrum and depleted pump spectrum while the OPO is operating at maximum power.

We investigated idler power scaling of the OPO, using a high reflector in place of M_8 to maximise the deep-IR power, with the results shown in Fig. 11. The pump power is corrected for a ~83% transmission loss through M_1. At a pump wavelength of 993 nm, the OPO threshold was measured to be ~340 mW, and the idler slope conversion efficiency is ~6.4 %, with a pump depletion of ~17%. As the threshold is higher than the theoretically calculated value (see [26] for method), it is clear that absorption processes in the crystal including two-photon absorption play a role in increasing the cavity losses.

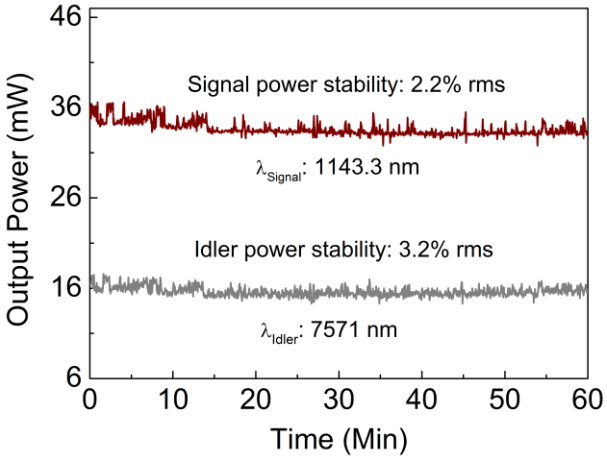

Fig. 12. Passive power stability of signal and idler at 1143.3 nm and 7571 nm, respectively, measured over 1 hour.

The passive power stability of signal and idler is shown in Fig. 12. At an idler wavelength of 7571 nm, the stability is estimated to be 3.2% rms over 1 hour, while the corresponding signal at 1143 nm exhibits a stability of 2.2% rms over the same period. Fig. 13 shows the spatial beam profiles of the signal and idler output from the OPO, recorded using a pyroelectric camera. As can be seen, both beams exhibit high spatial quality with single-peak TEM_{00} Gaussian distribution.

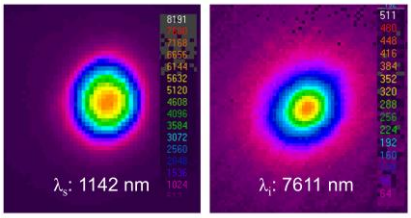

Fig. 13. Spatial beam profiles of the idler and signal at 7611 nm and 1142 nm, respectively.

We characterised the detailed spectral qualities of the signal and idler using two spectrum analysers for the near-IR and deep-IR with resolutions of 0.7 nm and ~4 nm, respectively. The signal spectra were found to be highly asymmetric, containing an SPM-induced long-wavelength tail, as expected for a cavity with a large net positive GVD. In

contrast, idler spectra were measured to be almost symmetric with evidence of atmospheric water absorption at shorter wavelengths in the form of deep modulations. In order to compare the relative brilliance of the OPO to other deep-IR sources, we calculated the spectral brightness as defined in [27], using data from Fig. 10. and Fig. 14. for an idler with waist radius w_{0i} = 18.0 μm and average power of 20 mW at 7314 nm. The calculation yields a value of 6.68×10^{20} photons s^{-1} mm^{-2} sr^{-1} 0.1% BW^{-1}, comparable to the record value from a mid-IR centred supercontinuum, and 2 orders of magnitude greater than a typical synchrotron facility [28, 29].

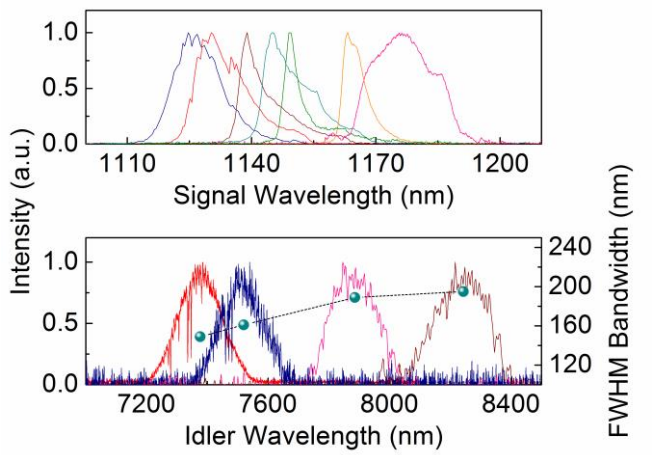

Fig 14. Signal and idler spectra, with idler FWHM bandwidths across the tuning range of the OPO.

The pulse duration was measured experimentally using an intensity autocorrelator, confirming strongly chirped pulses. Fig. 15 shows signal autocorrelation profiles and corresponding spectra at perfect synchronisation, (a) and (b), and when the cavity is slightly negatively detuned, (c) and (d). The autocorrelation measurements confirm durations of 319 and 259 fs, respectively, with corresponding spectra having approximate 10 dB bandwidths of 41.9 nm and 32.1 nm.

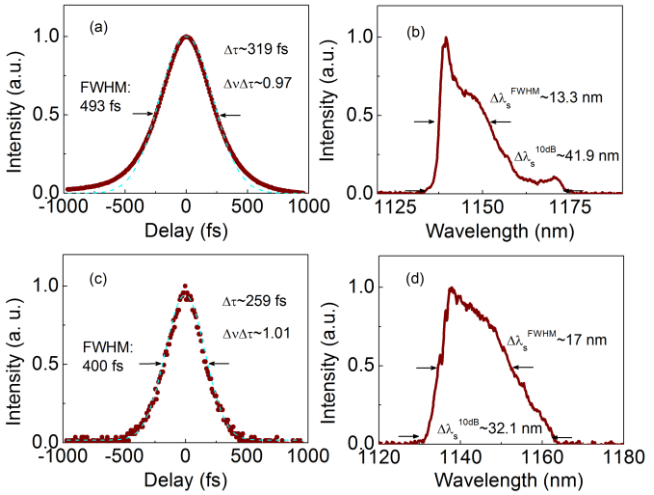

Fig. 15. Signal intensity autocorrelation at (a) perfect cavity synchronisation, with (b) corresponding spectrum. (c) Signal intensity autocorrelation with the cavity detuned, with (d) corresponding spectrum.

When the signal and pump pulses are not perfectly temporally overlapped, the reduced intracavity power induces a smaller nonlinear phase shift and results in a weaker pulse chirp. Therefore, since a strongly chirped pulse broadens rapidly under the influence of GVD, a shorter measured pulse duration away from synchronisation is consistent with intuition. This is also reflected in the respective corresponding spectra, of which the measurement at perfect synchronisation shows a wider 10 dB bandwidth, indicating stronger SPM effects. The results of Fig. 15(c) are compared to those predicted using a simple theoretical model of a signal pulse propagating in the presence of GVD, with higher order dispersion and nonlinear effects neglected. In this case the final pulse envelope is given by:

$$E(z,t) = \frac{1}{2\pi}\int_{-\infty}^{\infty} E(0,\omega)\exp\left(\frac{i\omega^2 GDD}{2} - i\omega t\right) d\omega \qquad (2)$$

Where $E(0,\omega)$ is the Fourier transform of the initial pulse envelope $E(0,t)$, which is assumed to have an intensity distribution of the form $P(0,t)\equiv|E(0,\ t)|^2=P_{peak}\cdot sech^2(t/\tau_0)$, where τ_0 is related to the pulse FWHM by $\tau_0=\Delta\tau/1.763$. If the initial signal pulse duration is set equal to that of the pump ($\Delta\tau_p$~137 fs), evaluating (2) gives a final signal pulse duration of $\Delta\tau_s$~263 fs, in strong agreement with the experimental observations in Fig. 15(c). A more realistic model could be obtained by applying the nonlinear Schrödinger equation (NLSE) to the circulating signal pulses. The general NLSE considers multiple-order dispersion, SPM, intrapulse Raman scattering, and self-steepening of the temporal profile [30]. However, in order to calculate the magnitude of the nonlinear effects, knowledge of the Kerr refractive index, n_2, of CSP is required, which, to the best of our knowledge, has not yet been determined. It is expected that including this term in our calculations would bring the predicted final pulse width closer to the experimentally measured value. Alternatively, deploying suitable intracavity dispersion compensation in the form of chirped mirrors, or a four prism compressor, would bring the time-bandwidth product closer to the transform limit.

IV. Conclusions

In conclusion, we have demonstrated a high-spectral-brilliance, high-repetition-rate femtosecond source of coherent radiation for the deep-IR using a single frequency conversion stage pumped by a KLM Ti:sapphire laser. By exploiting the wide transparency window of CSP, we have been able to achieve successful operation of a deep-IR femtosecond OPO directly using a KLM Ti.sapphire laser, for the first time. In doing so, we have produced up to 20 mW of average power at 7314 nm, equivalent to a spectral brightness of 6.68×10^{20} photons s^{-1} mm^{-2} sr^{-1} 0.1% BW^{-1}, with up to 37 mW generated in the near-IR signal. We have used three separate tuning methods; type-I critical phase-matching, pump wavelength tuning, and cavity delay tuning, to generate coherent radiation across 1127–1192 nm and 6654–8373 nm (1194–1503 cm^{-1}) in the signal and idler,

respectively, with typical FWHM spectral bandwidths of 140–180 nm in the deep-IR. In particular, exploiting the tunable properties of the Ti:sapphire laser has permitted rapid tuning of the deep-IR idler wavelength over key spectral regions, including the amide III band, of great interest for medical imaging. The signal and idler beams exhibit excellent TEM_{00} spatial quality and passive long-term power stability of 2.2% and 3.2% rms over 1 hour, respectively. Spectral and temporal characterisation of the signal has revealed chirped pulses with a time-bandwidth product, $\Delta\upsilon\Delta\tau\sim1$. Both the pulse durations and 10 dB spectral bandwidths were observed to be broader at higher intracavity powers, indicating strong intracavity self-phase-modulation, which could be reduced using appropriate intracavity dispersion management. With high average power at a high repetition rate, this OPO represents an attractive source for low-noise spectroscopy, frequency comb generation and medical diagnostics in the 6.5–8.5 μm spectral region, using a simplified pumping method based on established ultrafast KLM Ti:sapphire laser technology.

V. References

[1] H. Günzler, and H. U. Gremlich, *IR spectroscopy: An introduction*, Germany: Wiley-VCH, 2002.

[2] S. Dupont, C. Petersen, J. Thøgersen, C. Agger, O. Bang, and S. R. Keiding, "IR microscopy utilizing intense supercontinuum light source," *Opt. Express*, vol. 20, no. 5, pp. 4887–4892, Feb 2012.

[3] J. Hildenbrand, J. Herbst, J. Wöllenstein and A. Lambrecht, "Explosive detection using infrared laser spectroscopy," in *Proc. of SPIE OPTO 7222*, San Jose, California, USA, 2009, pp. 72220B.

[4] C. Petibois and G. Deleris, "Chemical mapping of tumor progression by FT-IR imaging: towards molecular histopathology," *Trends Biotechnol*., vol. 24, pp. 455–462, Aug 2006.

[5] G. Edwards, R. Logan, M. Copeland, L. Reinisch, J. Davidson, B. Johnson, R. Maciunas, M. Mendenhall, R. Ossoff, J. Tribble, J. Werkhaven and D. O'Day, "Tissue ablation by a free-electron laser tuned to the amide II band," *Nature*, vol. 371, pp. 416–419, Sep 1994.

[6] L. M. Mille, and R. J. Smith, "Synchrotrons versus globars, point-detectors versus focal plane arrays: Selecting the best source and detector for specific infrared microspectroscopy and imaging applications," *Vib. Spectrosc.*, vol. 38, no. 1, pp. 237-240, Jul 2005.

[7] J. Faist, *Quantum cascade lasers*, UK: OUP Oxford, 2013.

[8] C. R. Petersen, U. Møller, I. Kunbat, B. Zhou, S. Dupont, J. Ramsay, T. Benson, S. Sujecki, N. Abdel-Moneim, Z. Tang and D. Furniss, "Mid-infrared super-continuum covering the 1.4–13.3 μm molecular finger-print region using ultra-high NA chalcogenide step-index fibre," *Nat. Photonics*, vol. 8, no. 11, pp. 830–834, Nov 2014.

[9] M. Ebrahim-Zadeh and I. T. Sorokina, *Mid-infrared Coherent Sources and Applications*, Springer, 2008.

[10] M. Beutler, I. Rimke, E. Büttner, P. Farinello, A. Agnesi, V. Badikov, D. Badikov and V. Petrov, "Difference-frequency generation of ultrashort pulses in the mid-IR using Yb-fiber pump systems and AgGaSe2," *Opt. Express*, vol. 23, no. 3, pp. 2730–2736, Feb 2015.

[11] J. Krauth, A. Steinmann, R. Hegenbarth, M. Conforti, M, and H. Giessen, "Broadly tunable femtosecond near-and mid-IR source by direct pumping of an OPA with a 41.7 MHz Yb: KGW oscillator," *Opt. Express*, vol. 21, no. 9, pp. 11516–11522, May 2013.

[12] L. Kang, M. Zhou, J. Yao, Z. Lin, Y. Wu, and C. Chen, "Metal thiophosphates with good mid-infrared nonlinear optical performances: A first-principles prediction and analysis," *J. Am. Chem. Soc*., vol. 137, no. 40, pp. 13049–13059, Sep 2015.

[13] K. T. Zawilski, P. G. Schunemann, T. M. Pollak, D. E. Zelmon, N. C. Fernelius, and F. K. Hopkins, "Growth and characterization of large CdSiP2 single crystals," *J. Cryst. Growth*, vol. 312, no. 8, pp. 1127–1132, Apr 2010.

[14] S. Chaitanya Kumar, P. G. Schunemann, K. T. Zawilski, and M. Ebrahim-Zadeh, "Advances in ultrafast optical parametric sources for the mid-infrared based on CdSiP2," *J. Opt. Soc. Am. B*., vol. 33, no. 11, D44–D56, Nov 2016.

[15] A. Peremans, D. Lis, F. Cecchet, P. G. Schunemann, K.T. Zawilski, and V. Petrov, "Noncritical singly resonant synchronously pumped OPO for generation of picosecond pulses in the mid-infrared near 6.4 μm," *Opt. Lett*., vol. 34, no. 20, pp. 3053–3055, Oct 2009.

[16] O. Chalus, P. G. Schunemann, K. T. Zawilski, J. Biegert, and M. Ebrahim-Zadeh, "Optical parametric generation in CdSiP2," *Opt. Lett*., vol. 35, no. 24, pp. 4142–4144, Dec 2010.

[17] G. Marchev, A. Tyazhev, V. Petrov, P. G. Schunemann, K. T. Zawilski, G. Stöppler, and M. Eichhorn, "Optical parametric generation in CdSiP2 at 6.125 μm pumped by 8 ns long pulses at 1064 nm," *Opt. Lett.*, vol 37, no. 4, pp. 740–742, Feb 2012.

[18] Z. Zhang, D. T. Reid, S. Chaitanya Kumar, M. Ebrahim-Zadeh, P. G. Schunemann, K. T. Zawilski and C. R: Howle, "Femtosecond-laser pumped CdSiP2 optical parametric oscillator producing 100 MHz pulses centered at 6.2 μm," *Opt. Lett.*, vol. 38, no. 23, pp. 5110–5113 Dec 2013.

[19] S. Chaitanya Kumar, J. Krauth, A. Steinmann, K. T. Zawilski, P. G. Schunemann, H. Giessen and M. Ebrahim-Zadeh, "High-power femtosecond mid-infrared optical parametric oscillator at 7 μm based on CdSiP2," *Opt. Lett.*, vol. 40, no. 7, pp. 1398–1401, Apr 2015.

[20] V. Ramaiah-Badarla, S. Chaitanya Kumar, A. Esteban-Martin, K. Devi, K. T. Zawilski, P. G. Schunemann, and M. Ebrahim-Zadeh, "Ti: sapphire-pumped deep-infrared femtosecond optical parametric oscillator based on CdSiP2," *Opt. Lett.*, vol. 41, no. 8, pp. 1708–1711, Apr 2016.

[21] S. Chaitanya Kumar, A. Esteban-Martin, A. Santana, K. T. Zawilski, P. G. Schunemann, and M. Ebrahim-Zadeh, "Pump-tuned deep-infrared femtosecond optical parametric oscillator across 6–7 μm based on CdSiP2," *Opt. Lett.*, vol. 41, no. 14, pp. 3355–3358, Jul 2016.

[22] N. Leindecker, A. Marandi, R. L. Byer, K. L. Vodopyanov, J. Jiang, I. Hartl, M. Fermann and P. G. Schunemann, "Octave-spanning ultrafast OPO with 2.6-6.1 μm instantaneous bandwidth pumped by femtosecond Tm-fiber laser," *Opt. Express*, vol. 20, no. 7, pp. 7046–7053, Mar 2012.

[23] B. Metzger, B. Pollard, I. Rimke, E. Büttner, and M. B. Raschke, "Single-step sub-200 fs mid-infrared generation from an optical parametric oscillator synchronously pumped by an erbium fiber laser," *Opt. Lett*., vol. 41 no. 18, pp. 4383–4386, Sep 2016.

[24] L. Maidment, P. G. Schunemann, and D. T. Reid, "Molecular fingerprint-region spectroscopy from 5 to 12 μm using an orientation-patterned gallium phosphide optical parametric oscillator," *Opt. Lett*., vol. 41 no. 18, pp. 4261–4264, Sep 2016.

[25] P. Loza-Alvarez, C. T. A. Brown, D. T. Reid, W. Sibbett, and M. Missey, "High-repetition-rate ultrashort-pulse optical parametric oscillator continuously tunable from 2.8 to 6.8 μm," *Opt. Lett*., vol. 24 no. 21, pp. 1523–1525, Nov 1999.

[26] J. M. McCarthy, and D. C. Hanna, "All-solid-state synchronously pumped optical parametric oscillator," *J. Opt. Soc. Am. B.*, vol. 10 no. 11, pp. 2180–2190, Nov 1993.

[27] I. Pupeza, D. Sánchez, J. Zhang, N. Lilienfein, M. Seidel, N. Karpowicz, T. Paasch-Colberg , I. Znakovskaya, M. Pescher, W. Schweinberger, V. Pervak, E. Fill, O. Pronin, Z. Wei, F. Krausz, A. Apolonski, and J. Biegert, "High-power sub-two-cycle mid-infrared pulses at 100 MHz repetition rate," *Nat. Photonics*, vol. 9, no. 721, pp. 721–724, Nov 2015.

[28] P. Dumas, F. Polack, B. Lagarde, O. Chubar, J. L. Giorgetta, and S. Lefrançois, "Synchrotron infrared microscopy at the French Synchrotron Facility SOLEIL," *Infrared Phys. Techn.* vol. 49, no. 1, pp. 152–160, Sep 2006.

[29] Y. Yu, X. Gai, P. Ma, D. Choi, Z. Yang, R. Wang, S. Debbarma, S. Madden and B. Luther-Davies, "A broadband,

quasi-continuous, mid-infrared supercontinuum generated in a chalcogenide glass waveguide," *Laser Photonics Rev.*, vol. 8, no. 5, pp. 792–798, Sep 2014.
[30] G. P. Agrawal, *Nonlinear fiber optics*. USA: Academic press, 2007.

Callum Francis O'Donnell received the Master in Physics (MPhys) degree from the University of Manchester, U.K., in 2015. He is a Marie Skłodowska-Curie fellow currently pursuing the Ph.D. degree at ICFO-The Institute of Photonic Sciences in Barcelona, Spain, and at *Radiantis*, a company spun-out from ICFO in 2004 based on the research performed in the group of Majid Ebrahim-Zadeh. His research interests include nonlinear optics, in particular ultrafast frequency conversion sources in the infrared.

Suddapalli Chaitanya Kumar received the B.Sc. degree in mathematics, physics and electronics from Acharya Nagarjuna University, India, in 2003, and the M.Sc. degree in physics from Indian Institute of Technology Guwahati, India, in 2006. He was awarded PhD in photonics with "*Excellent Cum Laude with Honours"* at ICFO-The Institute of Photonic Sciences, Barcelona, Spain, in 2012, for his thesis on high-power, fiber-laser-pumped optical parametric oscillators from the visible to mid-infrared. He was a Postdoctoral Fellow at ICFO from 2012-2015 and Research Fellow from 2015-2017. Currently, he is a Torres y Quevedo Fellow at Radiantis. His research interests include fiber-based optical frequency conversion sources, and continuous-wave and ultrafast optical parametric oscillators (OPOs) from the ultraviolet to mid-infrared. He has co-authored more than 60 peer-reviewed and invited papers in leading international journals in Photonics, with over 800 citations, and has presented more than 90 contributed, post deadline and invited papers at major international conferences such as *CLEO-USA* and *CLEO-Europe*. Throughout his career, he has worked on several funded projects with active international collaborations, and some of his research works have been highlighted in *Laser Focus World* and *Nature Photonics*. He is a professional member of Optical Society of America (OSA), The International Society for Optics and Photonics (SPIE). He also served as international outreach project manager at the Knowledge and Technology Transfer office of ICFO during 2013-2015. He is the recipient of the ICFO PhD thesis award in 2013, Universitat Politècnica de Catalunya (UPC) extraordinary doctoral thesis award in 2014 for his outstanding contribution to applied research and participated in the prestigious 66th Lindau Nobel Laureate meeting, Germany, in 2016.

Kevin T. Zawilski is a Sr. Principal Physicist at BAE Systems, Technology Solutions in Merrimack, NH. Dr. Zawilski received his B.S. in Chemical Engineering from Bucknell University (1998), M.S. and PhD. in Materials Science and Engineering from Stanford University (2000, 2003). At Stanford he studied the fluid dynamics of mixing techniques applied to Bridgman crystal growth and worked on crystal growth of systems including lead magnesium niobate-lead titanate (PMNT) and $CdGeAs_2$. He has been at BAE Systems since 2003 where he has been a key contributor to the crystal growth processing and characterization of nonlinear materials including the bulk growth of $ZnGeP_2$ and $CdSiP_2$ using horizontal gradient freeze and the thick film growth of Optically Patterned GaAs (OPGaAs), GaAs, GaP, and $In_xGa_{(1-x)}As_2$. He has led technical efforts of research programs as well as led production efforts for crystal growth of $ZnGeP_2$ for use in laser systems, and has authored over 60 technical publications and several patents.

Peter G. Schunemann is a leading researcher in nonlinear optical materials for the last 30 years, authoring or co-authoring over 350 publications and 6 patents in the field. He received B.S. and M.S. degrees in Materials Science and Engineering from MIT in 1984 and 1987 before joining BAE Systems, where he has led a series of development efforts to produce unique NLO crystals for mid-infrared frequency conversion – both birefringent and quasi-phase-matched – exhibiting the highest nonlinear coefficients among known materials: these include $ZnGeP_2$, $AgGaSe_2$, $CdGeAs_2$, $CdSiP_2$, OP-GaAs, and most recently OP-GaP. His work on $ZnGeP_2$ in particular, a critical component for next generation laser-based infrared countermeasure (IRCM) systems, earned him the Jack L. Bowers Award in 1994 (the company's highest technical award), a Nova Award in 1995 (Lockheed Martin's highest honor for technical excellence), and the Association of Old Crows Technology Hall of Fame award in 2002. He is a Fellow of OSA, SPIE, and past president of the American Association of Crystal Growth (AACG).

Majid Ebrahim-Zadeh is an Institucio Catalana de Recerca i Estudis Avancats (ICREA) Professor at ICFO-The Institute of Photonic Sciences, Barcelona, Spain. He received his PhD from St Andrews University, UK, in 1989. He was a Royal Society of London Research Fellow at St Andrews from 1993 to 2001, and a Reader from 1997 to 2003. He has been active in the advancement of nonlinear optics and parametric sources for over 20 years. His research has led the realization of many new and innovative nonlinear frequency conversion sources from the UV to mid-IR and from the continuous-wave to femtosecond time-scales. He has published over 190 journal and 300 peer-reviewed conference papers, including 90 invited and 14 post-deadline presentations at major international conferences, has edited 2 books and authored 15 major invited book chapters and reviews in volumes such as *Science*, OSA *Handbook of Optics*, *Handbook of Laser Technology and Applications*, *and Laser and Photonics Reviews*. For over 20 years, he has been a regular instructor of short course on OPOs at *CLEO/USA* and *CLEO/Europe*, has served over 50 times as sub-committee chair and member of technical, organizing and steering committees of major conferences worldwide, and has chaired 7 international conferences and workshops. He has served as associate editor of *IEEE Photonics Journal*, as advisory and topical editor of *Optics Letters*, as guest editor of *J. Opt. Soc. Am. B*, and currently serves as an associate editor of *Optica*. Professor Ebrahim-Zadeh is the founder, president and chief scientist of *Radiantis*, and recipient of several honors and awards, including Royal Society of London university research fellowship and merit awards (UK), Innova Prize for technology innovation and enterprise (Spain), and Berthold Leibinger Innovation Prize (Germany). He is a Fellow of OSA and SPIE.